ARMY RESEARCH LABORATORY

Investigation of Chemical Processes Involving Laser-generated Nanoenergetic Materials

by Jennifer L. Gottfried

ARL-MR-0736 **February 2010**

NOTICES

Disclaimers

The findings in this report are not to be construed as an official Department of the Army position unless so designated by other authorized documents.

Citation of manufacturer's or trade names does not constitute an official endorsement or approval of the use thereof.

Destroy this report when it is no longer needed. Do not return it to the originator.

Army Research Laboratory
Aberdeen Proving Ground, MD 21005

ARL-MR-0736 **February 2010**

Investigation of Chemical Processes Involving Laser-generated Nanoenergetic Materials

Jennifer L. Gottfried
Weapons and Materials Research Directorate, ARL

REPORT DOCUMENTATION PAGE

Form Approved
OMB No. 0704-0188

1. REPORT DATE *(DD-MM-YYYY)*	2. REPORT TYPE	3. DATES COVERED (From - To)
February 2010	DRI	

4. TITLE AND SUBTITLE
Investigation of Chemical Processes Involving Laser-generated Nanoenergetic Materials (WMR-FY09-03)

5a. CONTRACT NUMBER

5b. GRANT NUMBER

5c. PROGRAM ELEMENT NUMBER

6. AUTHOR(S)
Jennifer L. Gottfried

5d. PROJECT NUMBER

5e. TASK NUMBER

5f. WORK UNIT NUMBER

7. PERFORMING ORGANIZATION NAME(S) AND ADDRESS(ES)
U.S. Army Research Laboratory
ATTN: RDRL-WMB-D
Aberdeen Proving Ground, MD 21005

8. PERFORMING ORGANIZATION REPORT NUMBER
ARL-MR-0736

9. SPONSORING/MONITORING AGENCY NAME(S) AND ADDRESS(ES)

10. SPONSOR/MONITOR'S ACRONYM(S)

11. SPONSOR/MONITOR'S REPORT NUMBER(S)

12. DISTRIBUTION/AVAILABILITY STATEMENT
Approved for public release; distribution unlimited.

13. SUPPLEMENTARY NOTES

14. ABSTRACT
The feasibility of a novel approach for studying the chemical reactions between metallic nanoparticles and molecular explosives has been demonstrated. This method is based on the production of nanoparticles in a laser-induced plasma and the simultaneous observation of the atomic and molecular emission characteristic of the species involved in the intermediate chemical reactions of the nanoenergetic material in the plasma. Time-resolved, broadband emission of chemical species involved in the reaction of RDX and various metal nanoparticles was observed. The increase in diatomic carbon (C_2) and aluminum monoxide (AlO) emission with increasing aluminum (Al) content previously observed during an aluminized-RDX explosion in a shock tube was confirmed using this method. The time-evolution of species formation in the plasma, the effects of laser pulse energy, and the effects of trace metal content on chemical reactions were also studied.

15. SUBJECT TERMS
nanoparticle formation, nanoenergetic materials, laser ablation, plasma chemistry, optical emission

16. SECURITY CLASSIFICATION OF:			17. LIMITATION OF ABSTRACT	18. NUMBER OF PAGES	19a. NAME OF RESPONSIBLE PERSON
a. REPORT	b. ABSTRACT	c. THIS PAGE			Jennifer L. Gottfried
Unclassified	Unclassified	Unclassified	UU	22	19b. TELEPHONE NUMBER (*Include area code*) (410) 306-0884

Contents

List of Figures

Acknowledgments

I wish to acknowledge the contributions of Dr. Frank C. De Lucia, Jr. (U.S. Army Research Laboratory, Weapons and Materials Research Directorate). Dr. De Lucia assisted with the experimental setup and provided helpful input on the experimental plan and data analysis.

INTENTIONALLY LEFT BLANK.

1. Objective

The feasibility of a novel approach for studying the chemical reactions between metallic nanoparticles and molecular explosives has been demonstrated. This method is based on the production of nanoparticles in a laser-induced plasma and the simultaneous observation of the time-resolved atomic and molecular emission characteristic of the species involved in the intermediate chemical reactions of the nanoenergetic material in the plasma.

2. Approach

It is essential to understand the chemical mechanisms of combustion, thermal explosion, and detonation in order to develop more efficient explosives and propellants. It is well known that two-component explosives consisting of metal particle fuels and oxidizers can produce more than twice as much energy as high performance molecular explosives alone (*1*).

Because of the high heat of formation for alumina (Al_2O_3), the addition of aluminum (Al) to explosive formulations results in a considerable increase in the heat of explosion. Al is rapidly oxidized by oxygen (O, O_2), carbon dioxide (CO_2), water (H_2O), and possibly other species such as nitric oxide (NO), nitrous oxide (N_2O), and nitrogen dioxide (NO_2) to form aluminum monoxide (AlO) before reaching its final equilibrium state, Al_2O_3 (*2*). Recently, the presence of Al was shown to promote the ejection process of carbon from the intermediate products of RDX pyrolysis, which decreases rocket propellant performance (*3*). Conventional formulations of energetic materials containing Al particles to improve the performance of explosives and propellants use particles with a mean diameter of ~30 μm, but nanoscale materials offer the possibility of faster energy release, more complete combustion, and greater control over performance (*1, 4*). The development of nanoenergetic materials has been hampered by the lack of fundamental knowledge of the chemical dynamics involved.

Previous experiments have demonstrated that ablation of an Al target with a pulsed laser produces Al nanoparticles with a mean primary particle size of 1–100 nm (depending on laser pulse duration and fluence as well as carrier gas type and pressure) (*5, 6*). Here, we have combined the ablation of thin-film residues of molecular explosives (~2.5 $\mu g/mm^2$) on Al substrates (generating nanoenergetic particles) with the observation of time-resolved optical emissions from the resulting high-temperature plasma. The relative concentrations of carbon (C), diatomic carbon (C_2), CN, Al, AlO, hydrogen (H), nitrogen (N), and O (as well as any other atomic, molecular, or ionic species emitting from 200–940 nm) were tracked during the lifetime of the plasma (typically <1 ms). Because the laser pulse duration is too short to directly initiate the explosives (<10 ns) and the heat deposited by the laser is rapidly conducted through the

substrate, detonation of the explosive material was not observed. The potential advantages to this approach include (1) little or no sample preparation is needed (the laser directly ablates the explosive and substrate material); (2) the intermediate chemical reactions of the nanoenergetic material can be studied on a small scale (microgram quantities), eliminating the need for a shock tube or other explosive containment apparatus; (3) the properties of the laser (pulse energy, wavelength, pulse duration) can be tuned to control the size and distribution of the particles formed; and (4) high-resolution, time-resolved relative concentrations of a large number of atomic and molecular species can be tracked simultaneously.

The first task was to confirm the results of Song et al. (*3*), who observed an increase in C_2 emission when the concentration of micro-aluminum powder (3–9 μm) was increased. Unlike the previous experiment, our experiment (1) did not require the use of a shock tube, (2) involved laser-generated nanometer-sized Al particles rather than commercial micrometer-sized particles, and (3) enabled us to track the relative concentrations of a large number of atomic and molecular species simultaneously. Previous work by McNesby and coworkers (*7*) demonstrated that the primary source of oxygen for the oxidation of an ablated Al target is from air, so in order to determine whether the Al nanoparticles are being oxidized by the decomposition products of the RDX or from the air, the experiments were carried out under an inert argon atmosphere as well.

The second task was to optimize the production of nanoparticles in the laser-induced plasma. Since the reactivity of the Al nanoparticles has been shown to increase with decreasing size (*8*), we would expect to see a difference in the emission intensities of the reaction species as the average size and distribution of the energetic materials in the plasma was varied. We compared the relative concentrations of the reaction species under different atmospheric conditions (air vs. argon) and at different laser pulse energies. The use of two successive nanosecond laser pulses (separated by a several μs delay), where the second laser pulse re-excites and further atomizes the ablated material (*9*), was also investigated.

The third task was to investigate other types of nanoenergetic materials. While the initial studies were performed with an RDX residue on an Al substrate, an additional 67 substrates were studied, including both pure metals (silver [Au], copper [Cu], indium [In], titanium [Ti], etc.) and metal alloys with known trace metal concentrations. In addition to observing the effect of trace metals on the plasma chemistry, commercially available Al powder was mixed with the RDX residue and added to non-Al substrates in order to determine the effect of the Al nanoparticles on the reaction chemistry. Finally, the chemical reactions of 10 different organic explosives (and 3 non-explosive organic materials) on an Al substrate were studied (*10*).

3. Results

Time-resolved emission spectra were acquired with an echelle/intensified charge-coupled device (ICCD) detector (Catalina Scientific SE200 and Apogee AP2Ep ICCD, t_{int}=1 µs) at various delays (t_{delay}) relative to the plasma generated using two Big Sky CFR400 lasers (2×225 mJ, Δt=2 µs). Emission spectra generated with a single-pulse laser in an argon atmosphere and a double-pulse laser in air were acquired. The wavelengths of the spectral lines in the emission spectra are characteristic of the excited atoms, ions, and molecules in the laser-induced plasma, while the intensity of the emitted light is proportional to the concentration of the emitting species. Although the relative emission intensities for the atomic and molecular species of interest were relatively constant for the first 6 µs of the plasma lifetime in the single-pulse argon plasma, the emission intensities for the double-pulse spectra at various delays showed some interesting trends. Figure 1 shows that as the continuum emission observed at t_{delay}=0 decreases with time, the atomic N, O, and H concentrations slowly decrease, the C concentration remains fairly constant, and the molecular species concentrations (CN, C_2, and AlO) increase as recombination reactions in the cooling plasma result in their formation. The excitation temperature, calculated from the Al emission lines using the Boltzmann method, decreases from about 7000 K at t_{delay}=0 to around 3700 K at t_{delay}=10 µs.

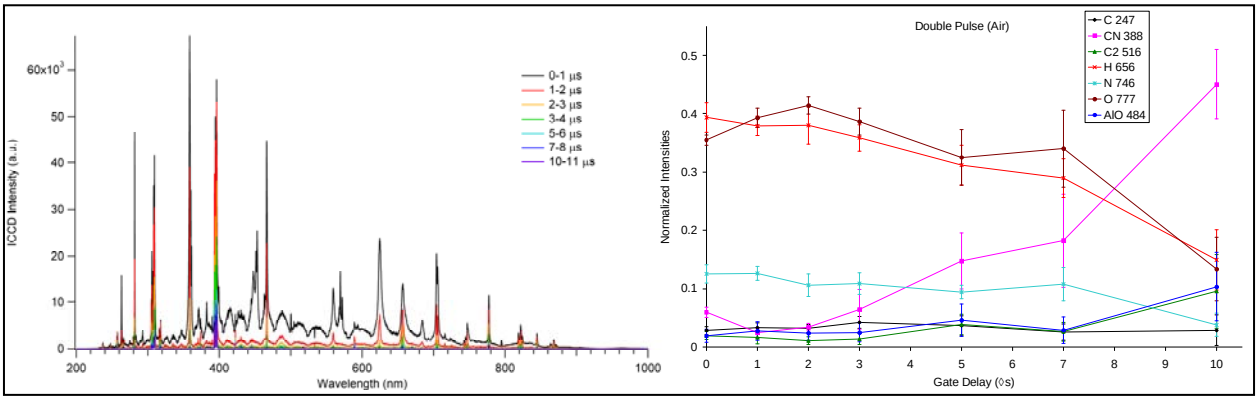

Figure 1. Time-resolved double-pulse spectra of RDX on Al in air at various delay times (left). While the concentration of atomic species slowly decreases over the first 11 µs (right), recombination reactions result in higher concentrations of CN, C_2, and AlO as the plasma cools.

The effect of laser pulse energy on the RDX/Al chemical reactions was studied using a Continuum Surelite laser system with an echelle/electron multiplying charge-coupled device (EMCCD) detector (Catalina Scientific EMU-65 and Andor iXon EMCCD, t_{delay}=1 µs, t_{int}=50 µs). Spectra of RDX on a high-purity Al substrate were acquired under argon with several laser ablation conditions: (1) 210 mJ single-pulse, (2) 420 mJ single-pulse, (3) 2×210 mJ double-pulse (Δt=2 µs), and (4) 2×420 mJ double-pulse (Δt=2 µs). The calculated excitation temperature of the plasma in all four cases is essentially identical (~8500 K). The emission spectra show that

increasing the laser energy from 210 to 420 mJ increased the overall spectral emission intensity and increased the relative AlO concentration (figure 2). The increase in AlO concentration is most likely a result of the higher reactivity of the Al particles in the plasma. A comparison of the single-pulse 420 mJ spectra and the double-pulse (420 mJ total) spectra shows that although the RDX signature is much stronger for the double-pulse ablation, the AlO emission decreases. Although double-pulse excitation produces smaller particle sizes, it also reduces the amount of atmospheric oxygen entrained in the laser-induced plasma (the argon gas flow reduces but does not eliminate atmospheric interference) (9). Therefore, there is less atmospheric O available to react with the Al in the double-pulse case (figure 2). Increasing the total double-pulse energy from 2×210 to 2×420 mJ results in an increase in AlO emission, as expected.

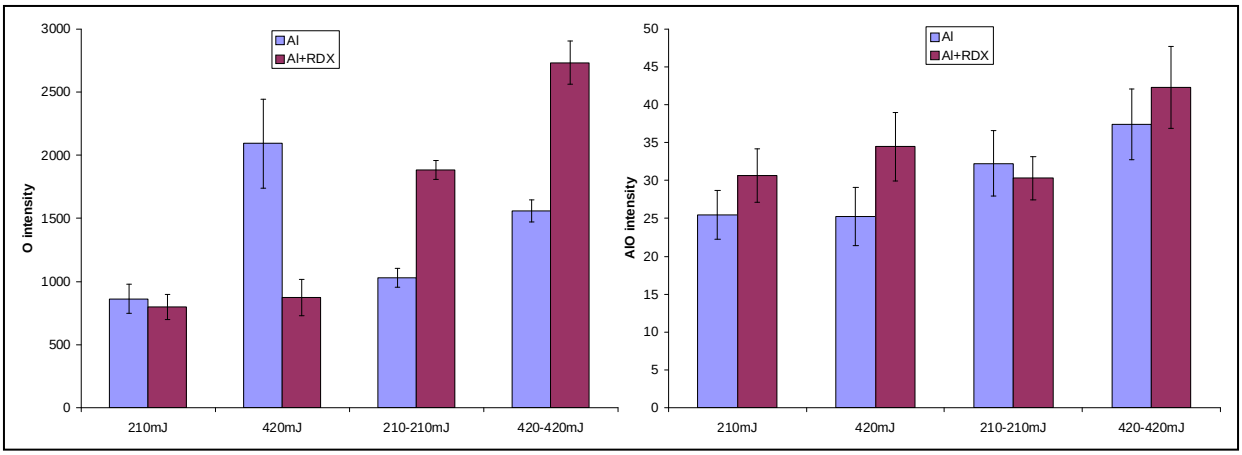

Figure 2. Comparison of O and AlO intensities for different laser pulse energies. The O in the blank Al spectra is primarily from residual atmospheric contributions. Error bars represent 95% confidence intervals.

Single-pulse spectra of 68 metal substrates were acquired in air with a LIBS2500+ 7-channel CCD spectrometer by Ocean Optics (200-940 nm, t_{delay}=1.5 µs, t_{int}=1 ms) using a Big Sky CFR400 laser (115 mJ) for the laser ablation and excitation. Samples surveyed included high-purity Al (99.999%), Cu (99.999%), nickel (Ni) (99.98%), tin (Sn) (99.998%), and Ti (99.998%) as well as numerous metal alloys including brass, lead, and steel. Differences in the spectra were observed based on trace element additives and impurities. For example, figure 3 shows the spectral differences observed in five Al-containing substrates. Comparison to the known trace element concentrations in the substrates confirmed the linear relationship between the observed emission intensities and elemental content. RDX residue dissolved in acetonitrile (2.5 µg/mm^2; ~1 µg of RDX sampled with each laser shot) was applied to a subset of the substrates surveyed, and double-pulse spectra under argon were acquired with the echelle/EMCCD detector (t_{delay}=1 µs, t_{int}=50 µs) from plasmas generated by the Continuum Surelite laser system (2×420 mJ, Δt=2 µs). Differences in the chemistry related to trace element content were observed (figure 4). The high-purity Al sample resulted in the strongest C and AlO emission intensity in the presence of RDX.

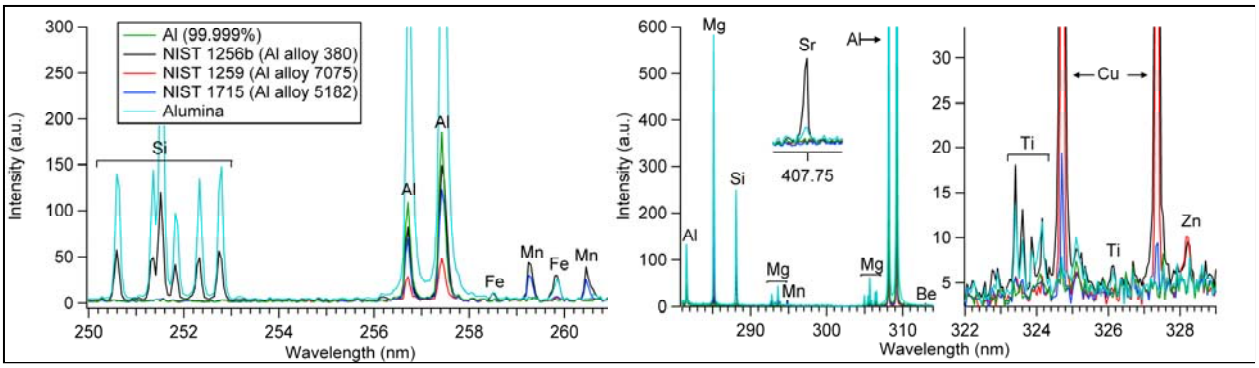

Figure 3. Selected regions of single-shot, single laser pulse emission spectra (in air) of high-purity Al, three National Institute of Standards & Technology (NIST) Al alloy standard reference materials of known elemental content, and alumina.

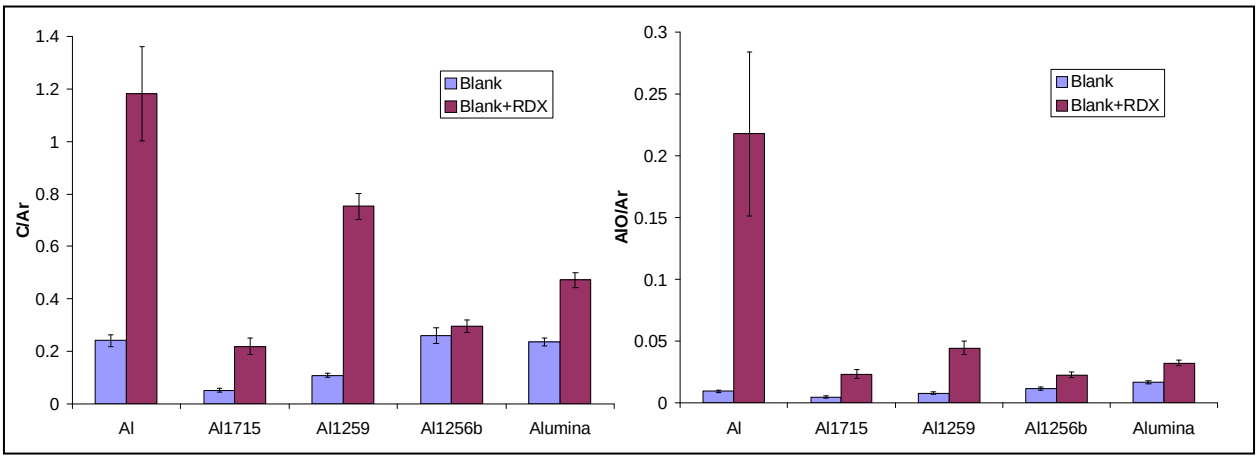

Figure 4. Carbon (left) and AlO (right) emission intensities (normalized to the argon line at 763 nm) for five Al substrates with and without RDX residue. Error bars represent 95% confidence intervals.

Selected regions of spectra from the five high-purity substrates with and without RDX (double pulse under argon) are shown in figure 5. The increase in the C, H, N, O, and CN emission with the presence of RDX (red traces) is clearly visible. The highest excitation temperatures of the RDX/metal plasmas correspond to Ti>Al>Cu>Sn>Ni. The extent of ionization in each plasma (represented by the ion/neutral ratio) follows the same trend as the temperature. The properties of the substrate have a clear effect on the chemistry of the RDX in the plasma, as shown in figure 6. The concentration of atomic O is highest in conditions of low C and low CN. This can be explained by the reaction of O with C or CN to form CO (and subsequently CO_2) via the following reactions (*11*):

$$C + O + M \rightarrow CO + M,$$
$$CN + O \rightarrow CO + N,$$
$$CO + O \rightarrow CO_2.$$

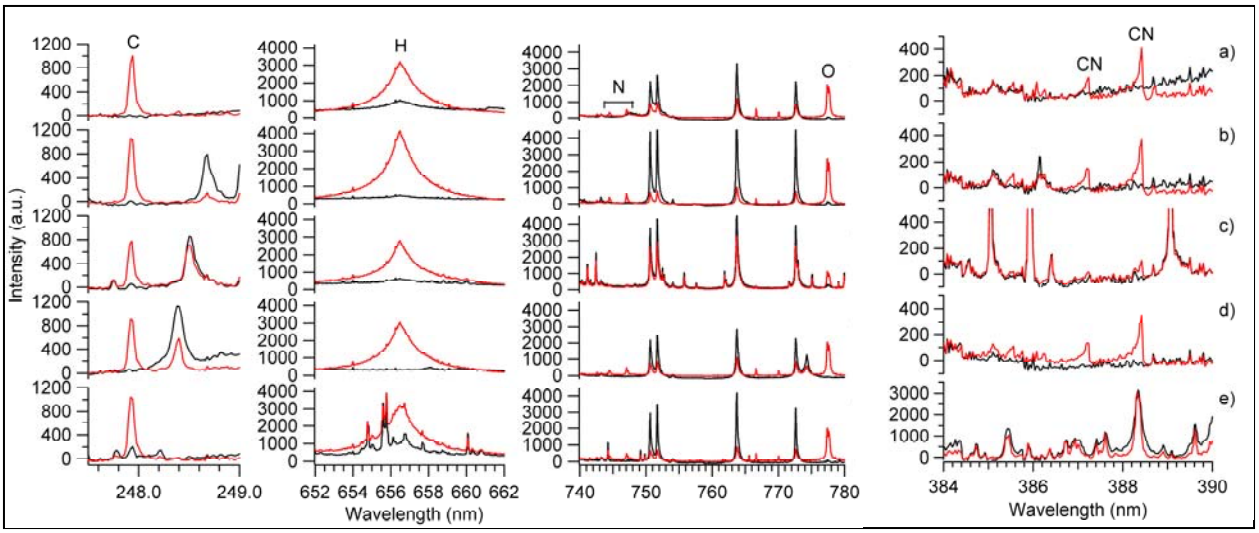

Figure 5. Selected regions of double-pulse spectra of a) Al, b) Cu, c) Ni, d) Sn, and e) Ti under argon with (red trace) and without (black trace) RDX. Unidentified lines correspond to argon or metal substrate emission.

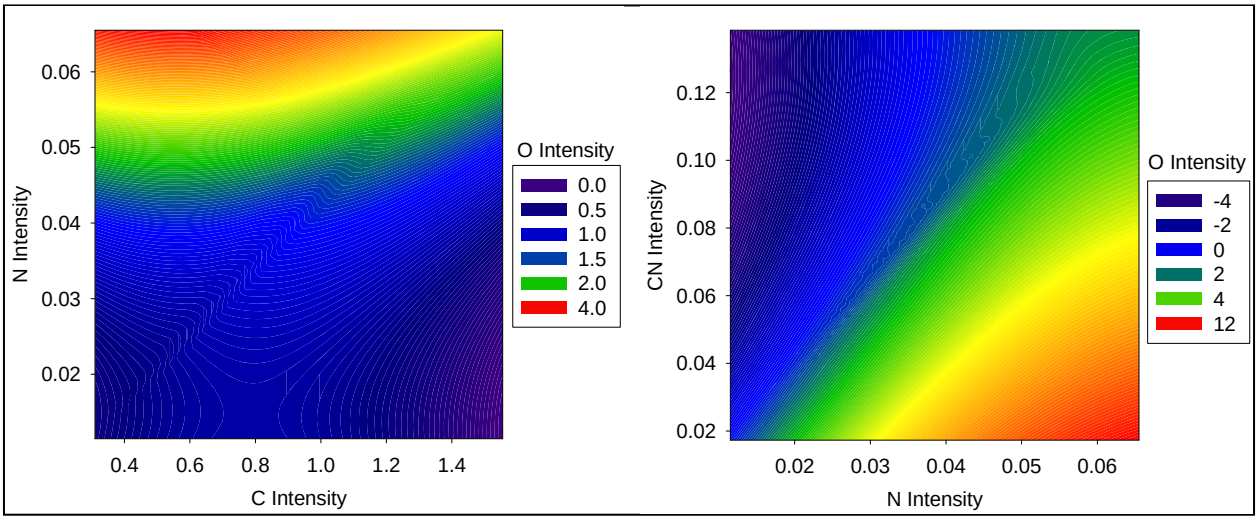

Figure 6. Contour plot of the C, N, and O (left) and N, CN, and O (right) emission intensities of RDX on five different metal substrates (Al, Cu, Ni, Sn, and Ti). The concentration of the O is decreased by the presence of C and CN.

The effect of Al on the chemistry of RDX was studied by mixing Al powder (<75 µm) with RDX in varying concentrations (1:0, 1:1, 1:2, and 1:4) and applying the RDX/Al mixture to the five high-purity substrates shown in figure 5. The plasma temperature for each substrate increased by as much as 50% with the addition of Al powder to the RDX. As the concentration of Al powder was increased, the substrate emission lines decreased and the Al emission lines increased (figure 7). While the C, H, N, H, and CN emission lines decreased with increasing Al, the C_2 and AlO increased on all substrates (figure 7). This result clearly confirms the conclusions of Song et al. (*3*), who observed the increase in C_2 and AlO emission with increasing Al content

during an aluminized-RDX explosion in a shock tube. The higher the concentration of Al in the plasma, the more O the Al scavenges to form AlO, and the less O available to react with the C to form CO. This results in an increase in condensed phase C aggregate (soot) and C_2.

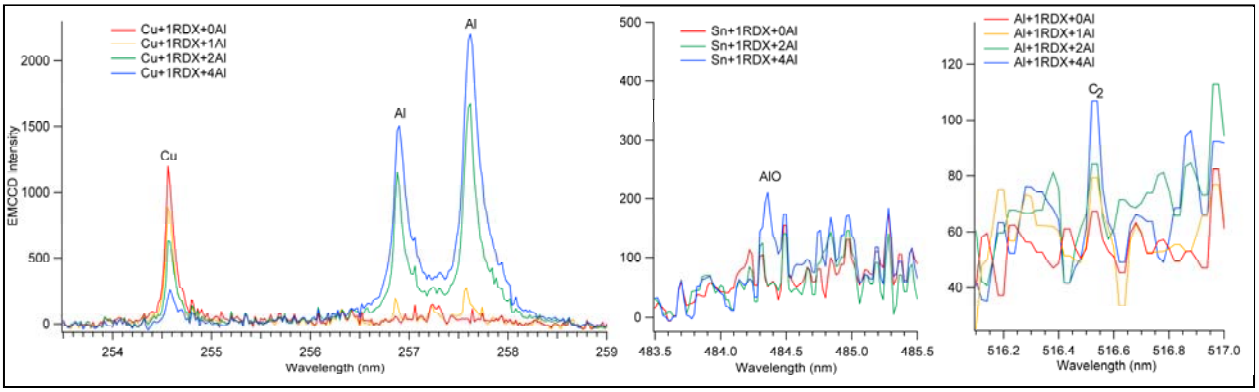

Figure 7. As the concentration of Al in the RDX/Al mixture was increased, the substrate emission lines decreased (due to increased residue surface coverage), and the Al, AlO, and C_2 emission lines increased.

4. Conclusions

Time-resolved, broadband emission of chemical species involved in the reaction of RDX and various metal nanoparticles was observed. The observations of Song et al. (*3*) were confirmed using the promising new methodology presented here for investigating the chemical processes involved in nanoenergetic material reactions. The time-evolution of species formation, the effects of laser pulse energy, and the effects of trace metal content on chemical reactions were studied. Future improvements to the experimental setup should include the incorporation of online monitoring of particle size distribution (*12*) and the monitoring of mid-IR emission from the plasma to obtain information on the concentration of important species such as CO, CO_2, NO, and NO_2 in the plasma (*13*). Additional experiments to be performed include tuning the laser properties such as pulse duration and wavelength to adjust the size and size distribution of the ablated particles, and exploring other explosive formulations such as TNT/Al, Al/Teflon, etc.

Although the optical emission spectroscopy of explosive materials has been used for the detection and identification of explosives (*14*), to the best of our knowledge, this work represents the first use of high-resolution optical emission to study the chemical reactions of energetic materials in laser-induced plasmas. This method provides the U.S. Army Research Laboratory (ARL) with new capabilities for nanoenergetic material evaluation and formulation, and has several advantages: (1) minimal sample preparation is required, (2) real-time, time-resolved analysis of chemical reaction intermediates can be achieved, (3) it uses small-scale, high-temperature reactions that do not require containment equipment, and (4) the ratio of fuel/oxidizer is not limited by the need to cast the explosive formulation. The chemical reactions

that occur between Al nanoparticles and explosives are not well understood. By monitoring the emission intensity of the different reactant species as a function of time, a better understanding of the chemistry of metallic nanoparticles and explosives at high temperatures could be achieved, eventually enabling the development of improved explosive formulations with higher explosive power and fewer harmful byproducts.

5. References

1. Yang, Y.; Sun, Z.; Wang, S.; Dlott, D. D. Fast Spectroscopy of Laser-Initiated Nanoenergetic Materials. *J. Phys. Chem. B* **2003**, *107* (19), 4485–4493.

2. Ji, Z.; Shufen, L. Aluminum Oxidation in Nitramine Propellant. *Propellants Explos. Pyrotech.* **1999**, *24* (4), 224–226.

3. Song, Y.; Jing-he, W.; Yan-ping, W.; Guo-dong, W.; Xiang-dong, Y. Optical Investigation of Shock-produced Chemical Products in Pseudo-aluminized Explosive Powders Explosion. *J. Phys. D* **2007**, *40*, 3541–3544.

4. Brousseau, P.; Anderson, C. J. Nanometric Aluminum in Explosives. *Propellants Explos. Pyrotech.* **2002**, *27* (5), 300–306.

5. Ullmann, M.; Friedlander, S. K.; Schmidt-Ott, A. Nanoparticle Formation by Laser Ablation. *J. Nano. Res.* **2002**, *4* (6), 499–509.

6. Amoruso, S.; Bruzzese, R.; Vitiello, M.; Nedialkov, N. N.; Atanasov, P. A. Experimental and Theoretical Investigations of Femtosecond Laser Ablation of Aluminum in Vacuum. *J. Appl. Phys.* **2005**, *98* (4), 044907.

7. Piehler, T. N.; DeLucia Jr., F. C.; Munson, C. A.; Homan, B. E.; Miziolek, A. W.; McNesby, K. L. Temporal Evolution of the Laser-induced Breakdown Spectroscopy Spectrum of Aluminum Metal in Different Bath Gases. *Appl. Opt.* **2005**, *44* (18), 3654–3660.

8. Park, K.; Lee, D.; Rai, A.; Mukherjee, D.; Zachariah, M. R. Size-resolved Kinetic Measurements of Aluminum Nanoparticle Oxidation with Single Particle Mass Spectrometry. *J. Phys. Chem. B* **2005**, *109* (15), 7290–7299.

9. Babushok, V. I.; De Lucia Jr., F. C.; Gottfried, J. L.; Munson, C. A.; Miziolek, A. W. Double Pulse Laser Ablation and Plasma: Laser Induced Breakdown Spectroscopy Signal Enhancement. *Spectrochim. Acta, Part B* **2006**, *61*, 999–1014.

10. De Lucia Jr., F. C.; Gottfried, J. L. Characterization of a Series of Nitrogen-rich Molecules Using Laser-induced Breakdown Spectroscopy. *Propellants, Explos., Pyrotech.*, submitted 2009.

11. Babushok, V. I.; DeLucia, F. C.; Dagdigian, P. J.; Gottfried, J. L.; Munson, C. A.; Nusca, M. J. ; et al. Kinetic Modeling Study of the Laser-induced Plasma Plume of Cyclotrimethylenetrinitramine (RDX), *Spectrochim. Acta, Part B* **2007**, *62B* (12), 1321–1328.

12. Sattari, R.; Dieling, C.; Barcikowski, S.; Chichkov, B. Laser-based Fragmentation of Microparticles for Nanoparticle Generation. *J. Laser Micro. Nanoengineer.* **2008**, *3* (2), 100–105.

13. Yang, C.S.-C.; Brown, E. E.; Hommerich, U. H.; Trivedi, S. B.; Samuels, A. C.; Snyder, A. P. Mid-infrared Emission from Laser-induced Breakdown Spectroscopy. *Appl. Spectrosc.* **2007**, *61* (3), 321–326.

14. Gottfried, J. L.; De Lucia Jr., F. C.; Munson, C. A.; Miziolek, A. W. Laser-induced Breakdown Spectroscopy for Detection of Explosives Residues: A Review of Recent Advances, Challenges, and Future Prospects. *Anal. Bioanal. Chem.* **2009**, *395*, 283.

6. Transitions

Manuscripts in preparation include (1) a detailed comparison and analysis of the 68 substrates studied in this work and (2) a comprehensive evaluation of the effects of laser pulse energy and atmospheric contributions. In addition, this experimental method has been applied to the study of the chemical reactions of other explosives besides RDX, including TNT and eight novel high-nitrogen explosives (*10*).

List of Symbols, Abbreviations, and Acronyms

Al	aluminum
Al_2O_3	alumina
AlO	aluminum monoxide
ARL	U.S. Army Research Laboratory
Au	silver
C	carbon
C_2	diatomic carbon
CO_2	carbon dioxide
Cu	copper
EMCCD	electron multiplying charge-coupled device
H	hydrogen
H_2O	water
ICCD	intensified charge-coupled device
In	indium
N	nitrogen
N_2O	nitrous oxide
NIST	National Institute of Standards & Technology
NO	nitric oxide
NO_2	nitrogen dioxide
O	oxygen
Sn	tin
Ti	titanium

No. of Copies	Organization
1 ELEC	ADMNSTR DEFNS TECHL INFO CTR ATTN DTIC OCP 8725 JOHN J KINGMAN RD STE 0944 FT BELVOIR VA 22060-6218
1 CD	US ARMY RSRCH LAB ATTN RDRL CIM G T LANDFRIED BLDG 4600 ABERDEEN PROVING GROUND MD 21005-5066
3 CDS	US ARMY RSRCH LAB ATTN IMNE ALC HRR MAIL & RECORDS MGMT ATTN RDRL CIM L TECHL LIB ATTN RDRL CIM P TECHL PUB ADELPHI MD 20783-1197
12 CDS 4 HCS	US ARMY RSRCH LAB RDRL WML A F DE LUCIA (1 HC, 1 CD) J GOTTFRIED (1 HC, 1 CD) W OBERLE (1 HC, 1 CD) RDRL WML B R PESCE-RODRIGUEZ (1 HC, 1 CD) B HOMAN J MORRIS RDRL WML C S AUBERT K MCNESBY RDRL WML D M NUSCA M MCQUAID RDRL WMP P BAKER RDRL WM B FORCH ABERDEEN PROVING GROUND MD 21005-5066

TOTAL: 21 (1 ELEC, 4 HCS, 16 CDS)

INTENTIONALLY LEFT BLANK.